

Article

Numerical and Experimental Investigation of Recycled Brick Coarse Aggregate Concrete

Yongcheng Ji ^{*}, Dayang Wang and Lifeng Wang ^{*}

School of Civil Engineering, Northeast Forest University, Harbin 150040, China

^{*} Correspondence: yongchengji@126.com (Y.J.); lifengwang2022@126.com (L.W.)

Abstract: This paper investigates the mechanical and micro-interfacial properties of recycled concrete. Concrete specimens with recycled brick coarse aggregate (RBCA) admixtures of 0%, 25%, 50%, 75%, and 100% were prepared. Apparent density, slump, and mechanical tests were carried out to evaluate the properties and behavior of the recycled concrete. The evolution laws of parameters such as compressive strength, peak strain, and elastic modulus of the recycled concrete specimens were tested and analyzed. Combined with numerical analysis, the stress distribution and damage propagation process of recycled concrete specimens with different RBCA contents were revealed. Furthermore, the RBCA content parameters and the thickness of the interface transition zone were analyzed to predict the mechanical behavior of RBCA concrete. The results show that the slump of fresh recycled concrete is less than 50 mm when the content of RBCA exceeds 50%. The apparent density of concrete is 15.55% lower than that of ordinary concrete when the content of RBCA is 100%. The cube compressive strength of RBCA concrete decreases with increased RBCA content. With increasing RBCA substitution rate, the internal cracks change from discrete to concentrated. The substitution rate of RBCA and thickness of the interfacial transition zone are negatively correlated with compressive strength and positively correlated with elastic modulus and peak stress.

Keywords: mechanical performance; random aggregate model; damage mechanism; mesoscopic mechanics; recycled aggregate concrete



Citation: Ji, Y.; Wang, D.; Wang, L. Numerical and Experimental Investigation of Recycled Brick Coarse Aggregate Concrete. *Appl. Sci.* **2022**, *12*, 9035. <https://doi.org/10.3390/app12189035>

Academic Editor: Luís Picado Santos

Received: 19 August 2022

Accepted: 6 September 2022

Published: 8 September 2022

Publisher's Note: MDPI stays neutral with regard to jurisdictional claims in published maps and institutional affiliations.



Copyright: © 2022 by the authors. Licensee MDPI, Basel, Switzerland. This article is an open access article distributed under the terms and conditions of the Creative Commons Attribution (CC BY) license (<https://creativecommons.org/licenses/by/4.0/>).

1. Introduction

Concrete is the most widely used construction material in engineering construction [1]. China's total commercial concrete production reached 2.843 billion cubic meters in 2020 [2]. However, the coarse aggregate which forms the skeleton of concrete is a non-renewable resource, and its exploitation leads to resource depletion and environmental pollution. Furthermore, construction waste pollutes the water, air, and soil, which is not conducive to the development of urban construction. An effective way to avoid this is to use construction waste to produce recycled concrete aggregate. Research on using recycled concrete coarse aggregate (RCCA) instead of natural coarse aggregate (NCA) has made significant progress in the past decade, and several standard specifications, including GB/T25177-2011 and GB/T25176-2011, have been completed. The RCCA concrete research mainly focuses on construction waste aggregates such as rubber, ceramic, red brick, cement, and foam [3]. In addition, a large amount of brick construction waste exists in China's urban and rural areas as a result of urbanization and development [4,5]. Therefore, the cyclic utilization of recycled brick coarse aggregate (RBCA) is significant to energy conservation and emission reduction in China.

When a brick building reaches the end of its service life, it is demolished, which generates waste bricks generated. Currently, most of the removed bricks are used in landfills and roadbeds, which causes waste of resources and creates environmental problems. RBCA can partially or fully replace the natural crushed coarse aggregate in concrete. The research and utilization of RBCA have greatly improved the utilization of brick resources, saved

non-renewable natural gravel, and protected the environment. RBCA is obtained by crushing waste bricks with a jaw crusher followed by screening, cleaning, and oven drying. Brick particles with particle sizes between 75 μm and 4.75 mm are defined as recycled fine aggregates, while those with particle sizes greater than 4.75 mm are recycled coarse aggregates [6]. RBCA with larger particle sizes has a flat and angular appearance; the aggregate surface is relatively rough, with many voids. RBCA with smaller particle sizes has many angles, rough surfaces, and microcracks. Currently, recycled brick aggregate is mostly used in non-load-bearing structures such as concrete pavement blocks [7] and porous concrete bricks [8].

Current research shows that low RCCA content influences recycled concrete's physical and mechanical properties [9–13], with the compression strength reduced by up to 30% after 100% replacement of raw aggregate (coarse aggregate) by RCCA [14]. RBCA has higher non-uniform composition than RCCA. In recent years, studies have been conducted to evaluate the compressive and working performance of RBCA concrete. For example, Awall et al. [15] studied the physical performance of concrete replaced by ordinary bricks and by over-fired bricks, including the unit weight of hardened concrete and the slump value of freshly mixed concrete. The results showed that the unit weight of concrete decreases with increasing coarse aggregate content of over-fired bricks, and the unit weight reached at least 79% of the regular unit weight of concrete. Bheel et al. [16] studied recycled concrete with a 100% waste brick replacement rate and evaluated its slump, density, compressive strength, and flexural strength. Zhang et al. [17] investigated waste brick aggregate concrete's functional performance and mechanical properties with different dosages. Research results have concluded that the operational performance is better if the dosage is less than 40% and that 30% recycled aggregate concrete meets the requirements of the strength standard. Poon et al. [18] discussed the influence of the moisture state of recycled aggregate on concrete performance, finding that recycled concrete with 100% air-dried recycled aggregate had severe slump loss. Agrela et al. [19] found that RBCA content significantly impacted the water absorption and dry density of the saturated surface of mixed recycled coarse aggregate. Jian et al. [20] experimentally studied the NCA replacement of concrete with different ratios of RBCA. The results showed that the mechanical properties of RBCA concrete exerted no significant decline when the replacement rate was less than 20%. However, the mechanical properties of RBCA concrete decreased significantly when the replacement rate was up to 50% and above. All of these observations concluded that the addition of RBCA reduces the performance of recycled aggregate.

In order to improve the application of RBCA concrete, scholars have studied the stress–strain relationship of RBCA concrete to support the structural design of recycled concrete and the numerical simulation calculation of recycled concrete. Chen et al. [21] tested the influence of red brick aggregate content on the mechanical properties of recycled red brick concrete. The red brick replacement rate parameter was introduced to correct the existing stress–strain relationship of recycled red brick concrete and a corrected stress–strain equation was presented. Ma et al. [22] established the constitutive damage model of recycled coarse aggregate concrete based on the Weibull function and equivalent strain principle. The constitutive relationship was modified by combining distribution and substitution rate functions. The presented model was able to satisfy the stress–strain relationship of recycled concrete with different mix and replacement ratios. Hu et al. [23] defined four characteristic points of a typical hysteresis loop according to experimental testing and established the constitutive equation of RAC under cyclic loading. Wei et al. [24] proposed a uniaxial compression damage constitutive model of recycled aggregate concrete considering the recycled aggregate replacement rate. Peng et al. [25] introduced the shape parameter of the stress–strain curve to present a theoretical stress–strain relationship considering the strength and replacement rate of reclaimed coarse aggregate.

Finite element numerical simulation can be used to numerically simulate the testing process, reducing the required test specimens and allowing more parameters to be investigated. Researchers have recently studied recycled concrete's mechanical properties and

crack damage through experiments and finite element models. For example, Wittmann et al. [26] proposed a stochastic aggregate model for simulating the failure mechanism of concrete in order to predict the mechanical behavior of recycled concrete. Zhou et al. [27] simulated the crack propagation process and mechanical properties of recycled concrete uniaxial compression specimens according to the damage plastic method of concrete. Jayasuriya et al. [28] presented a computational modeling method for controllable regenerative aggregate shape parameters, which was then mapped to the finite element model through an image analysis program. This method can more accurately simulate the arbitrary aggregate shape and aggregate distribution. Liu et al. [29] randomly placed concrete materials using the Monte Carlo method. They used a finite element model to analyze the uniaxial compression fracture of reinforced concrete with recycled aggregate content of 0%, 40%, 70%, and 100%. Ying et al. [30] obtained the macroscopic stress–strain relationship and failure process of RAC under uniaxial stress based on the three-dimensional finite element method. Yang et al. [31] used finite element software ABAQUS to simulate recycled concrete and study the mechanical differences between ordinary concrete and recycled concrete. Peng et al. [32] established a stochastic convex aggregate recycled concrete model and evaluated the uniaxial compressive strength and damage process of RCCA.

While there are many mechanical properties and mesoscopic mechanics of RCCA concrete, there have been relatively few studies on RBCA recycled concrete. RBCA concrete is made by replacing natural coarse aggregate in concrete with RBCA. Concrete specimens with RBCA content of 0%, 25%, 50%, 75%, and 100% were made for this study. The apparent density, slump, and cubic compressive strength of RBCA concrete with each content were measured, and the influence law of RBCA content on recycled concrete’s physical and mechanical properties was analyzed. In addition, ABAQUS was used to establish the random aggregate model of RBCA recycled concrete for mesonumerical simulation, and the experimental test results verified the accuracy of the proposed model. The replacement rate of recycled aggregate on the strength and elastic modulus was studied through the verification model, and the influence of the thickness of the interface transition zone on the strength of recycled concrete was analyzed. As a result, the mechanical properties of recycled concrete containing 20%, 40%, 60%, 80%, and 100% RBCA were predicted.

2. Materials and Methods

2.1. Materials

Ordinary concrete consists of cement, coarse aggregate, sand, water, and other materials. The cement used here was 42.5 grade ordinary Portland cement. The sand was local medium sand with a fineness modulus of 2.36, and the average particle size was 0.35–0.5 mm. Coarse aggregate included NCA and RBCA. First, waste red bricks were collected from construction waste sites. Second, the red brick was broken by a small jaw crusher in the laboratory. Finally, the crushed aggregate was screened, cleaned, and dried to obtain RBCA with a 5–20 mm particle size range. The NCA was ordinary gravel with a 5–20 mm particle size range. Table 1 describes the physical properties of the aggregates. Figure 1 shows the RBCA production process, including the collection site of the waste red bricks, the crushing process, and the crushed coarse aggregate with particle sizes of 10–20 mm and 5–10 mm. Compared with natural aggregate, the red brick aggregate is a flake with high water absorption, and micro-cracks can be observed on the aggregate surface.

Table 1. Physical properties of aggregate.

Raw Material	Apparent Density/(kg/m ³)	Bulk Density/(kg/m ³)	Water Absorption/%	Crush Value/%
RBCA	2190	990	18.61	32.9
NCA	2769	1543	1.45	14.8
Medium sand	2689	1655	0.51	/

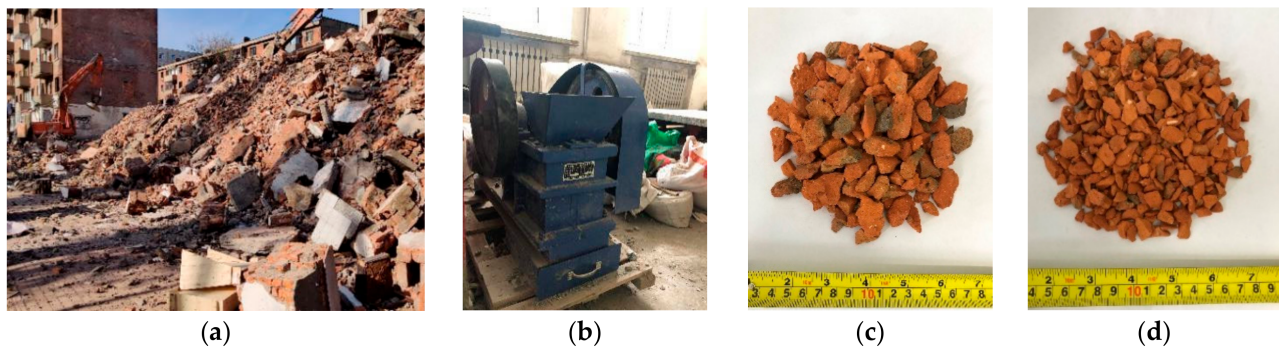


Figure 1. Collecting RBCA: (a) construction waste site, (b) broken red bricks in the laboratory, (c) 10~20 mm particle size, (d) 5~10 mm particle size.

The coarse and fine aggregate was mixed following the corresponding mass proportion. The grading curves of NCA and RBCA were located within the continuous grading interval in the specification, which meets the requirements of 5–20 mm continuous particle size. The grain gradation curve of the coarse aggregate is shown in Figure 2.

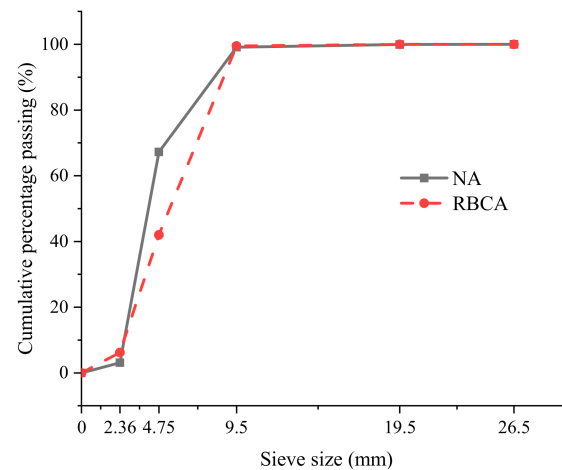


Figure 2. Particle gradation curve of coarse aggregate.

2.2. Specimen Preparation

The NCA concrete design strength was 30 MPa. Five RBCA volume replacement ratios were selected: 0, 25%, 50%, 75%, and 100%. The RBCA mass ratio was 3 to 7 for particle sizes from 5–10 mm to 10–20 mm. Table 2 shows the various mix designs of RBCA concrete.

Table 2. Mix designs of recycled concrete.

Group	Water (kg/m ³)	Cement (kg/m ³)	Gravel (5–10 mm) (kg/m ³)	Gravel (10–20 mm) (kg/m ³)	Sand (kg/m ³)	RBCA (5–10 mm) (kg/m ³)	RBCA (10–20 mm) (kg/m ³)
RB-0	195	487	341.5	796.5	613	0	0
RB-25	195	487	256.5	597.5	613	67.5	157.5
RB-50	195	487	170.5	398.5	613	135	315
RB-75	195	487	85.5	199.5	613	202.5	472.5
RB-100	195	487	0	0	613	270	630

Note: “RB” indicates RBCA concrete and “-number” indicates the corresponding percentage of RBCA added to concrete.

Cement, sand, natural aggregate, and recycled aggregate were weighed according to the RBCA concrete mix design calculation results (Table 2). The mixture was mixed evenly and added with water. The concrete was poured into the mold and placed on a shaking table for vibration. The concrete specimen was taken out after 24 h and immediately placed

in a standard curing chamber with 95% humidity and a temperature of 20 ± 2 °C for 28 days. The mechanical test was carried out after 28 days of curing time. Figure 3 shows a typical RBCA concrete specimen.

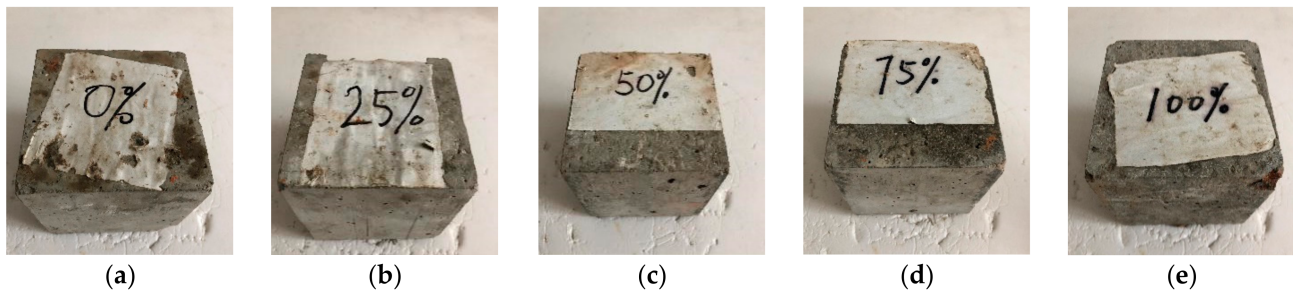


Figure 3. RBCA concrete specimens: (a) RB-0, (b) RB-25, (c) RB-50, (d) RB-75, (e) RB-100.

2.3. Compression Test

The test specimen dimensions were 100 mm by length, 100 mm by width, and 100 mm by height. The slump and apparent density of fresh concrete were tested according to National Standard GB/T 50080-2016. In addition, the compressive strength of concrete was tested according to National Standard GB/T 50081-2019. Figure 4 shows the microcomputer controlled electrohydraulic servo universal compression testing machine; the loading speed was 0.6 MPa/s. The experiment consisted of five categories, with three identical specimens in each category to guarantee data consistency.

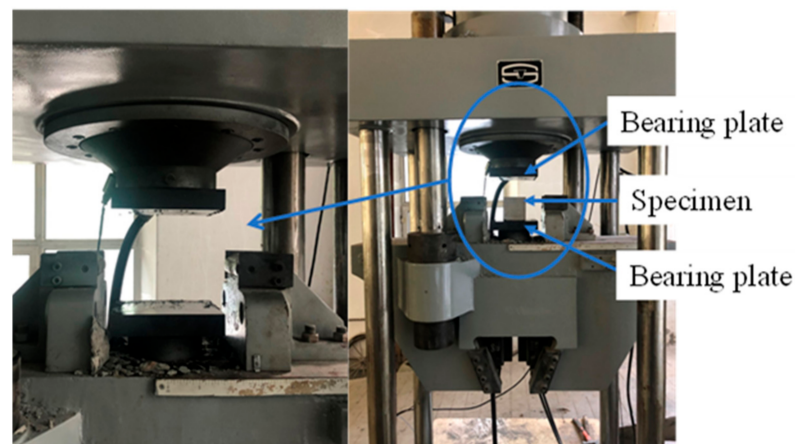


Figure 4. Microcomputer controlled electrohydraulic servo universal testing machine.

2.4. Numerical Simulation on RBAC Uniaxial Compress Test

Concrete is a three-phase composite material consisting of aggregate, mortar, and the interface between aggregate and mortar. Fine aggregate and coarse aggregate accounted for 60% to 75% of the total volume of concrete, of which coarse aggregate accounts for 40% to 50% [33]. In order to obtain the internal damage process and morphology of concrete under external load and other factors, a finite element model of random recycled aggregate was presented to reflect the concrete microstructure. The random aggregate algorithm was written based on Python, and the modeling and numerical analysis of two-dimensional recycled aggregate concrete were conducted using ABAQUS. Concrete was graded in three levels, and the thickness of the interface transition zone was determined at 0.5 mm in the numerical simulation [34].

Figure 5 shows the load and boundary conditions of the model, and the model dimension is 100 mm by length and 100 mm by width. Vertical constraints were set at the bottom of the model and horizontal constraints at the bottom's midpoint to simulate the

specimen’s bottom constraints in the compression test. A displacement load of -0.05 mm was applied on the top to simulate the compression of the loading plate of the testing machine. A total of 23,480 CPS3 units with an average size of 1.0 mm were used to mesh the mortar matrix, aggregate, and interface transition zone. Furthermore, mortar matrix, aggregate, and interfacial transition zone were connected by merging.

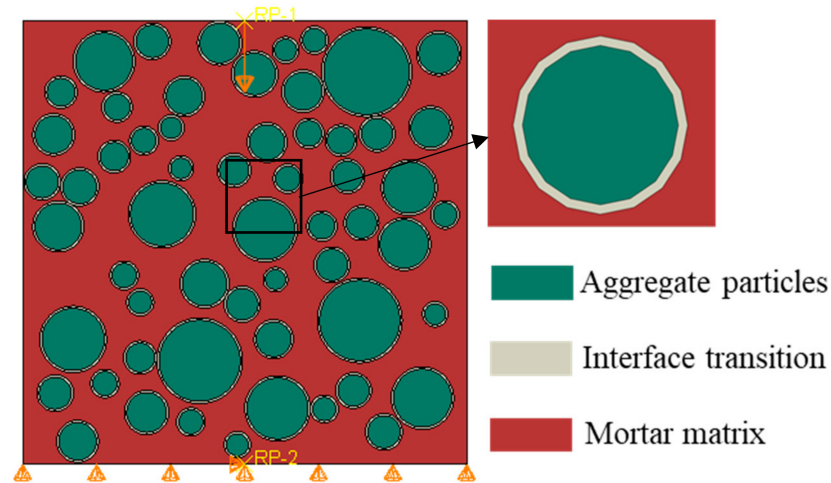


Figure 5. Two-dimensional mesonumerical model.

The mechanical behavior of the mortar matrix and the interface transition zone was similar to the mechanical behavior of concrete [21,22]. The plastic damage constitutive relationship of concrete proposed by Lee and Fenves [35] was adopted to describe its mechanical behavior in this study. RBCA is characterized by a rough surface, sharp edges, high water absorption, and low strength [36–38]. The failure mode of RBCA concrete is different from that of ordinary concrete, mainly existing in the mortar matrix and interface transition zone. The aggregate itself can be crushed and fractured. Research on RBCA’s constitutive relationship has previously been carried out. The modified plastic damage intrinsic model proposed in the literature [21] is used in this paper to describe the damage behavior of red brick particles. The constitutive formula adds the parameter r to consider the content of recycled aggregate, which is more accurate for numerical simulation of RBCA concrete. Furthermore, the elastoplastic constitutive relation is adopted for NCA concrete and has high strength.

The constitutive model of RBCA concrete is as follows:

$$\sigma = E_r \varepsilon \exp \left[1 - \left(\frac{\varepsilon}{a} \right)^b \right] \quad (1)$$

The total damage variable D of recycled concrete with different replacement levels:

$$D = 1 - \frac{E_r}{E_0} \exp \left[- \left(\frac{\varepsilon}{a} \right)^b \right] \quad (2)$$

$$a = \frac{\varepsilon_p}{\left(\frac{1}{b} \right)^{\frac{1}{b}}} \quad (3)$$

$$b = \frac{1}{\ln \left(\frac{E_r \varepsilon_p}{\sigma_p} \right)} \quad (4)$$

In Formulas (1) and (2), E_0 is the elastic modulus of concrete with a 0% recycled aggregate replacement rate, E_r is the elastic modulus of concrete with a replacement rate of $r\%$, and the parameters a and b are distribution parameters of the Weibull distribution, which can be obtained by combining the peak strain with Formulas (3) and (4).

It is necessary to determine the mechanical parameters of three-phase materials (RBCA particles, mortar matrix, and interfacial transition zone) in the mesoscopic numerical simulation of RBCA concrete.

The mechanical parameters are defined as in the code ‘Concrete plastic constitutive model (CDP) requirements and relevant provisions (GB50010-2010)’, which includes eccentricity, yield surface coefficient K , and viscosity parameters of recycled concrete.

In addition, the mechanical parameters such as mortar matrix, interface transition zone, elastic modulus E , compressive strength, and tensile strength of aggregate are determined [28,29,39]. Because of its high strength, NCA does not break the ring in the uniaxial compression test of concrete. Only its compressive and tensile strength parameters need to be defined. Table 3 shows the mechanical parameters of each mesoscopic component.

Table 3. Material parameters.

Material Phase	RBCA [39]	NCA [28]	Mortar Matrix [29]	Interfacial Transition Zone [39]
Poisson’s ratio ν	0.20	0.16	0.2	0.2
dilatancy angle ψ (°)	30	/	30	15
f_{b0}/f_{c0}	1.16	/	1.16	1.16
K	0.66667	/	0.66667	0.66667
Viscosity coefficient	1×10^{-5}	/	1×10^{-5}	1×10^{-5}
Eccentricity (%)	0.1	/	0.1	0.1
Compressive strength (MPa)	18	144	28.96	16
Tensile strength (MPa)	5.1	9.6	1.988	1.6
Elastic modulus (MPa)	16,000	70,000	28,960	26,000

3. Results and Discussion

RBCA has a lighter mass and higher water absorption than NCA. Therefore, the replacement rate of RBCA changes the physical properties of concrete. In addition, the bonding of RBCA and NCA with cement mortar is different. In addition, the average particle size and substitution rate of RBCA affect the flow performance of recycled concrete [40]. Therefore, the microstructure and mechanical performance of RBCA with different substitution rates were studied and compared.

3.1. Slump

Figure 6 shows the variation trend of recycled aggregate content on workability. When fresh concrete is mixed, the RBCA is in a water retaining state and the aggregates are surface-wet. Compared with the slump of RB-0, the slump of RB-25, RB-50, RB-75, and RB-100 decreased by 29%, 71.3%, 86.2%, and 90%, respectively. The slump decreases significantly when the recycled aggregate replacement rate is less than 50%. In addition, when the replacement rate exceeds 50% and the slump is less than 5 cm, the concrete presents a dry and hard state with poor workability.

According to standard code GB50164-92, RBCA concrete is a plastic and fluid concrete with an RBCA content of less than 50%. However, the performance of concrete is poor when the content of RBCA is more than 50%. Similarly, according to code JGJ/T10-2019, the slump of pumped concrete is required to be greater than 100 mm. Therefore, when the content of RBCA is less than 50%, the application range of recycled concrete is more extensive. The high water absorption, large inclination, and rough surface of RBCA are the main reasons for the decrease in a slump. However, previous studies have found that adding RBCA leads to reduced workability [14,15]. The solution to this problem is pre-soaked CBP or superplasticizers [40,41].

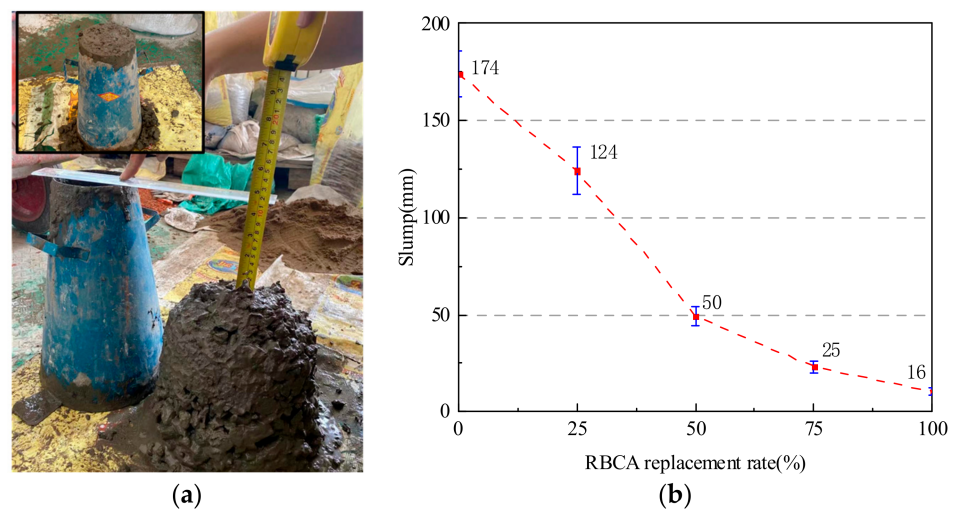


Figure 6. Slump test of concrete: (a) Slump test, (b) Slump of recycled concrete with different red brick content.

3.2. Apparent Density

Figure 7 shows the experimental results of the apparent density of fresh concrete. Apparent density is a material's mass ratio to its apparent volume. The apparent concrete density larger than 2800 kg/m^3 is regarded as heavy concrete, and smaller than 1950 kg/m^3 is light concrete. With increasing RBCA replacement rate, the apparent concrete density decreased from 2380 kg/m^3 to 2010 kg/m^3 . Concrete with 100% RBCA is close to the apparent density of lightweight concrete. Compared with the control category, the apparent density of RBCA concrete mixed with 25%, 50%, 75%, and 100% decreased by 3.95%, 7.52%, 10.46%, and 15.55%, respectively. It can be concluded that RBCA concrete is lightweight, which can be used in applications that require light quality and low-strength structural members.

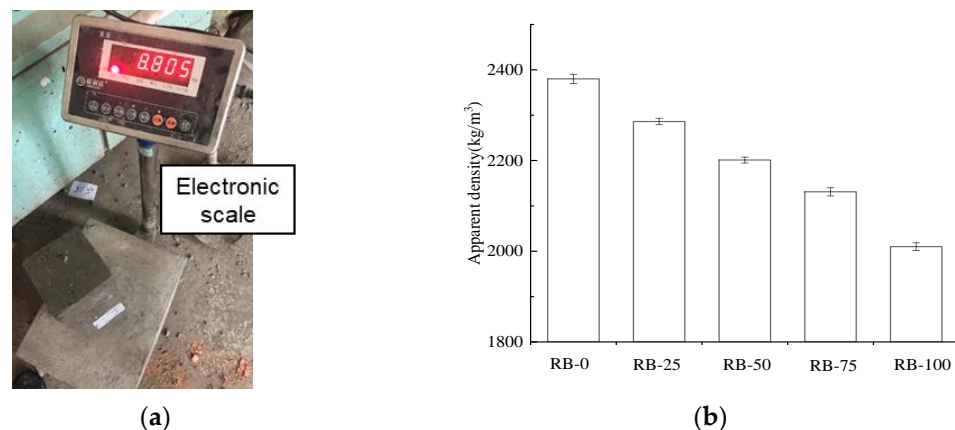


Figure 7. Apparent density of concrete experiment: (a) Apparent density test, (b) Apparent density of recycled concrete with different red brick contents.

3.3. Compressive Strength

Figure 8 shows the concrete failure mode during the compression test with different RBCA contents. It can be observed that the integrity of the concrete gradually decreased after compression failure with increasing RBCA contents. Due to its low strength, the RBCA was destroyed during the concrete compression process. However, more aggregate damage occurs in recycled concrete with increased RBCA content, which reduces the integrity of RBCA concrete.

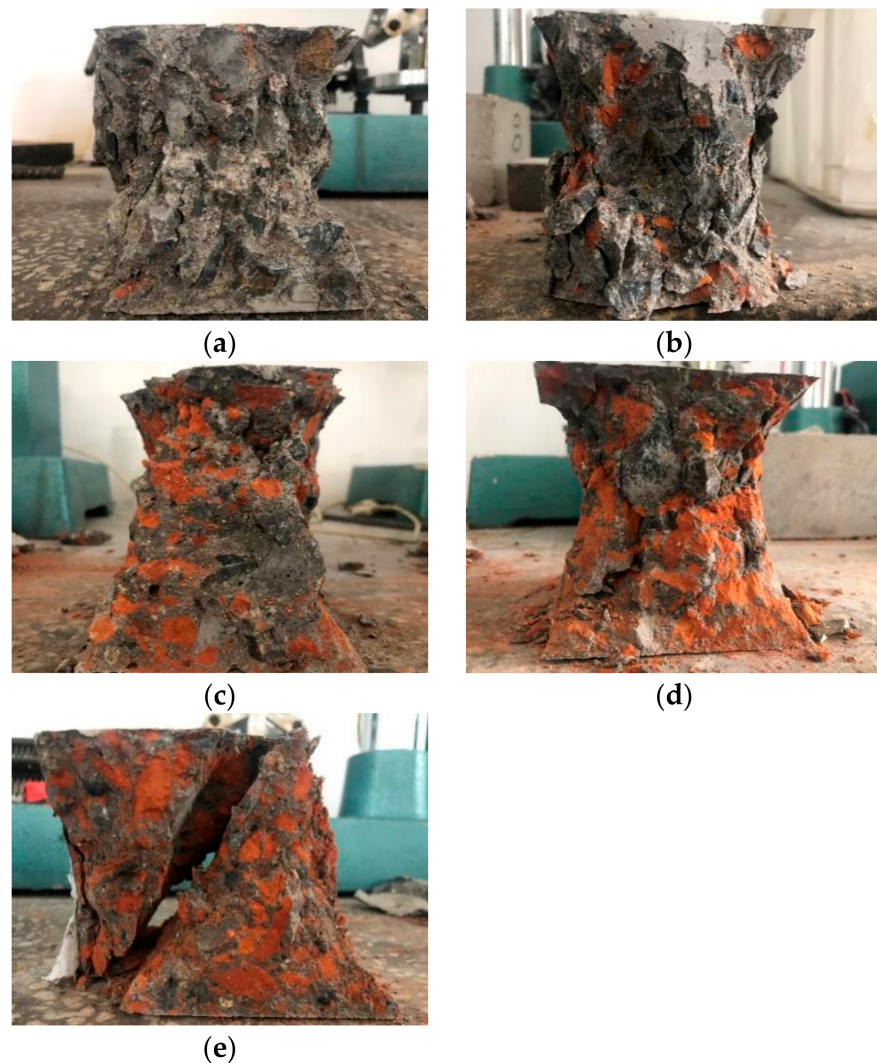


Figure 8. Compression failure mode of RBCA concrete specimens: (a) RB-0, (b) RB-25, (c) RB-50, (d) RB-75, (e) RB-100.

Figure 9 shows the RBCA concrete compressive strength test results for the five different aggregate replacement ratios. It can be observed that the concrete stress–strain relationship with different RBCA substitution rates has similar development patterns and shows apparent continuity and smoothness. The concrete compressive strength was decreased by 5.7%, 14%, 20.6%, and 28.6% when adding 25%, 50%, 75%, and 100% RBCA, respectively. Similarly, the concrete's peak strain increased from 2.5% to 15.0%, and the elastic modulus decreased from 10.4% to 38.5%, respectively. It can be observed that the maximum concrete compressive strength is close with RBCA contents from 0% to 50%, while the concrete compressive strength with RBCA contents of 75% and 100% decreased significantly. The RBCA concrete's peak compressive stress is always lower than ordinary concrete. Therefore, it can be concluded that increasing the RBCA content can reduce the strength and brittleness of concrete. The reason for this is that red brick aggregate is a high bibulous rate, low intensity, and porous material; these properties lead to the damage process of recycled concrete being different from that of traditional concrete. The damage process of recycled concrete occurs at the interface between the mortar and aggregate mortar as well as in the aggregate itself.

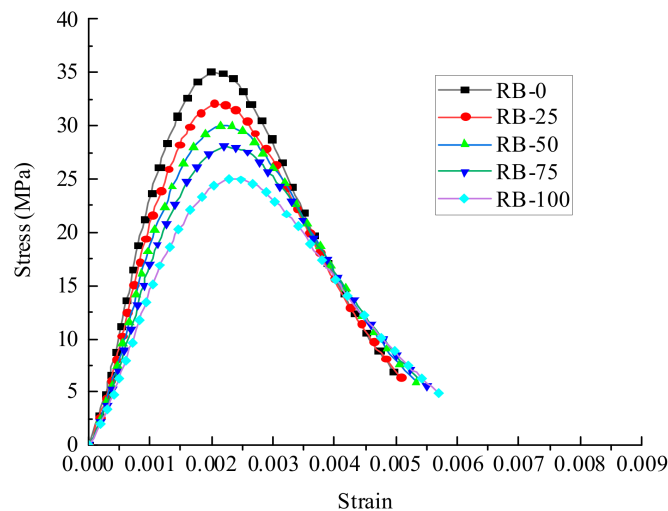


Figure 9. RBCA concrete stress–strain curve.

3.4. Calibration of the Numerical Model

3.4.1. Stress–Strain Relationship

Figure 10 shows the finite element model of RBCA concrete, with the green circle representing RBCA and the dark green circle representing NCA. The mechanical parameters were used to conduct a two-dimensional mesoscopic numerical simulation, as shown in Table 3. Figure 11 shows the calculated stress–strain curves of RB-0, RB-50, and RB-100, respectively. Compared with the experimental values of RB-0, RB-50, and RB-100, the errors of the calculated peak strength were 4.2%, 5.0%, and 6.1%. Similarly, the errors of the peak strain were 4.5%, 3.8%, and 4.3%, and the errors of the elastic modulus were 10.5%, 10.3%, and 11.4%, respectively. It can be seen that the numerical simulation results are relatively consistent with the experimental stress–strain relationship. However, the compressive strength, peak strain, and elastic modulus are slightly higher than the simulation values. All these observations can be attributed to the lower strength of red brick is compared to that of the mortar matrix and to the uniaxial compressive strength of RBCA concrete being between the strength of the mortar matrix and red brick. Therefore, both the mesoscopic method's feasibility and the rationality of parameter selection are preliminarily verified.

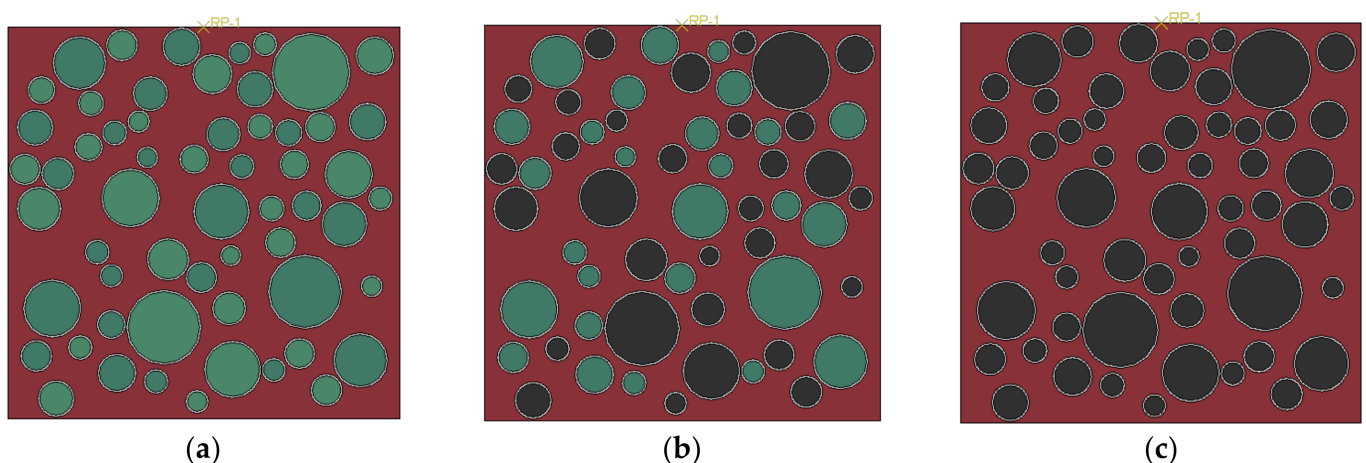


Figure 10. Two-dimensional finite element model (Note: ■ RBCA ■ NCA). (a) RB-100, (b) RB-50, (c) RB-0.

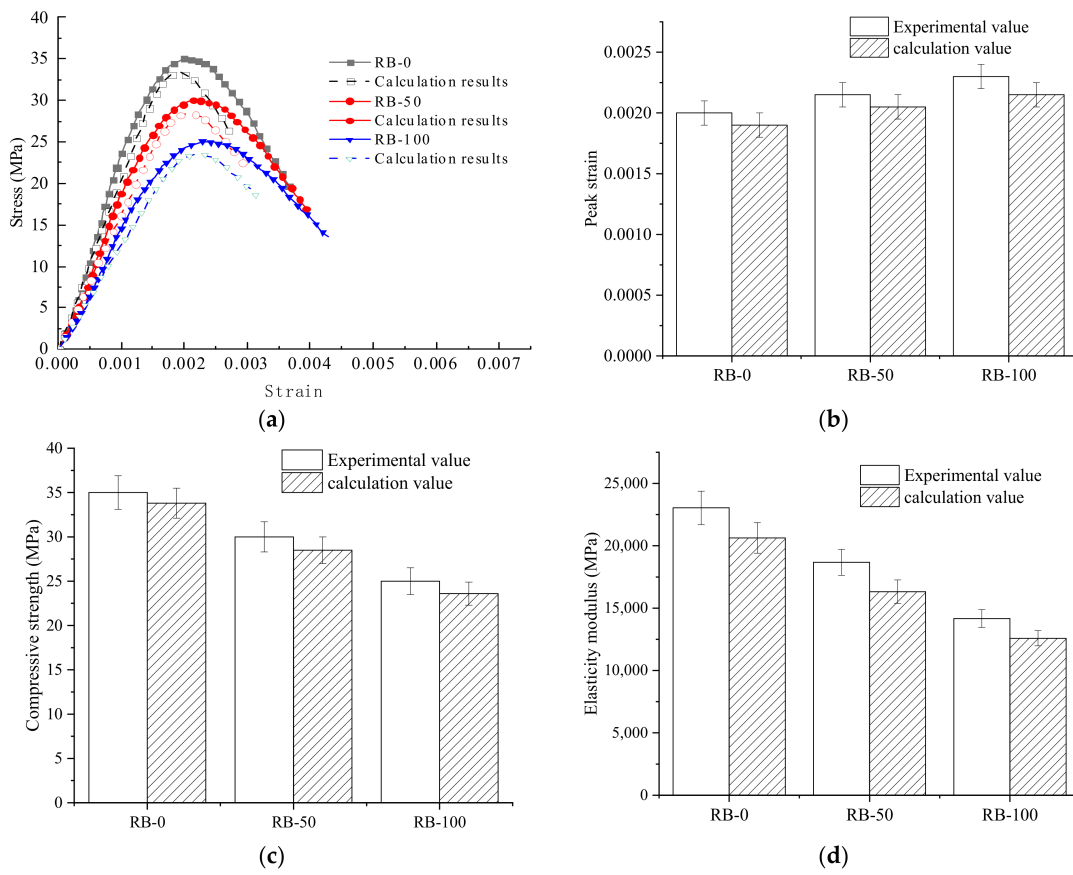


Figure 11. Comparison between numerical simulation and test results: (a) stress–strain curve, (b) histogram of peak strain, (c) histogram of compressive strength, (d) histogram of elastic modulus.

3.4.2. Uniaxial Compression Failure Behavior

A digital microscope was used to observe the specimen and its falling fragments after uniaxial compression failure, as shown in Figure 12a. Figure 12b,c shows the failure state of the samples after uniaxial compression of the two aggregates. Figure 12d shows the shape of cracks on the surface of the recycled concrete. It can be observed that the RBCA itself is damaged, the interface transition zone and mortar matrix are damaged, RCCA is not damaged, and there are V-shaped cracks on the surface of the recycled concrete. These phenomena are further verified in Table 4.

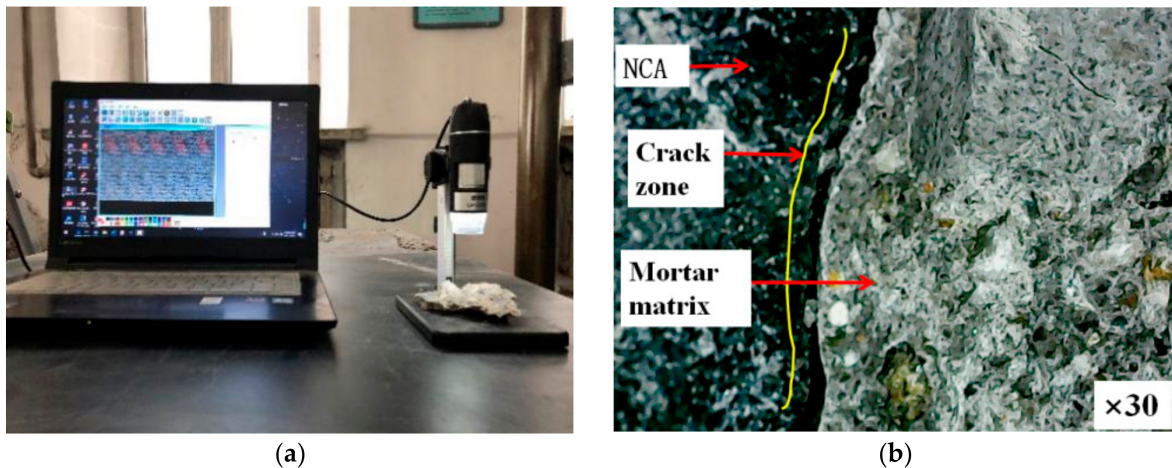


Figure 12. Cont.

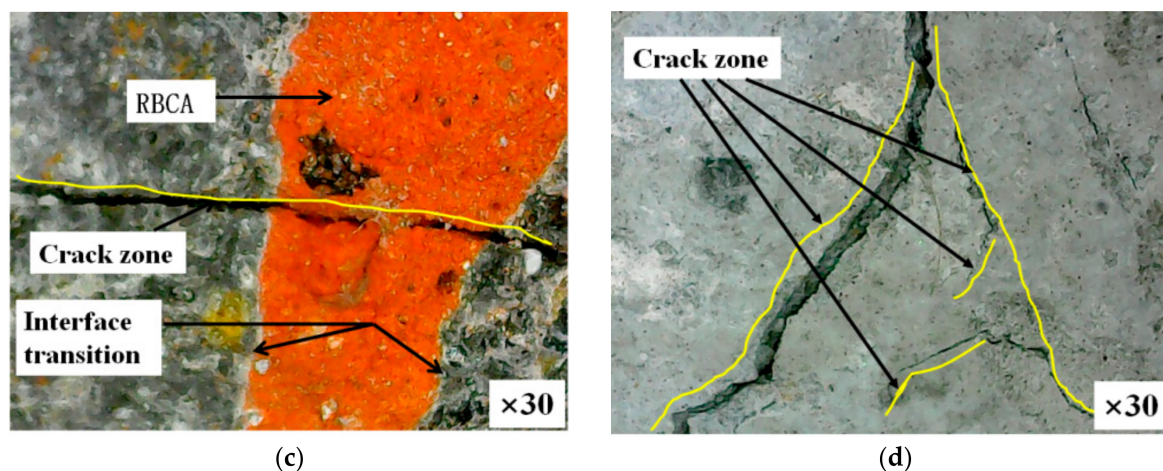


Figure 12. Destruction state of the specimen after uniaxial compression: (a) microscope, (b) destruction state of RCCA under a 30× microscope, (c) destruction of RBCA under a 30× microscope, (d) destructive state of the specimen under a 30× microscope.

According to Figure 12 and Table 4, the damage development of RBCA concrete differs from that of ordinary concrete. RBCA concrete and ordinary concrete damage initially appear in the interface transition zone. After all the damage occurs in the transition zone of ordinary concrete, a V-shaped central damage zone is usually formed and develops towards the mortar zone. However, the damage to RBCA concrete occurred to the aggregate itself, and no central damage zone formed.

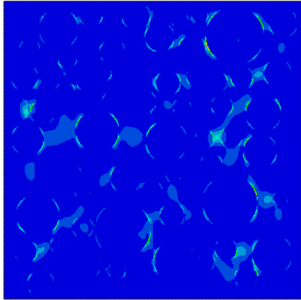
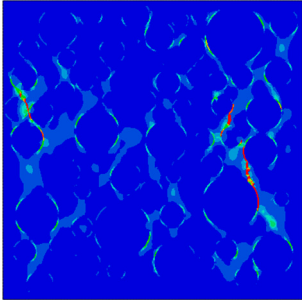
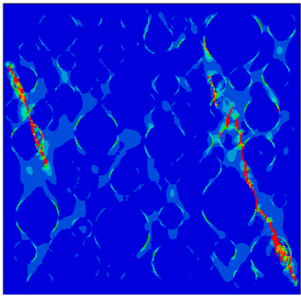
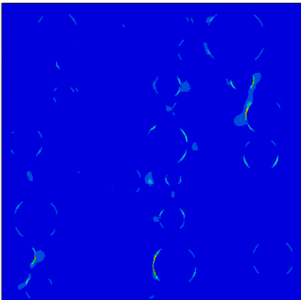
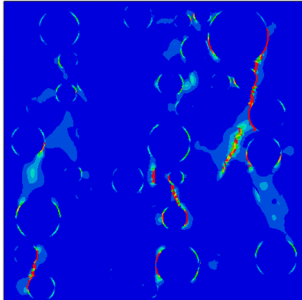
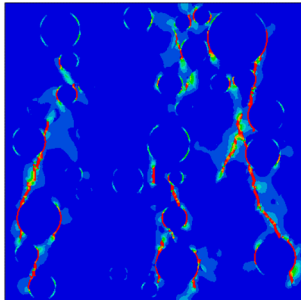
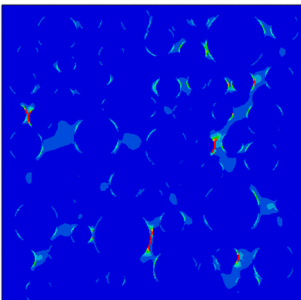
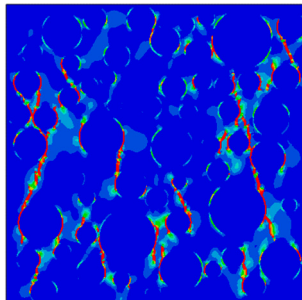
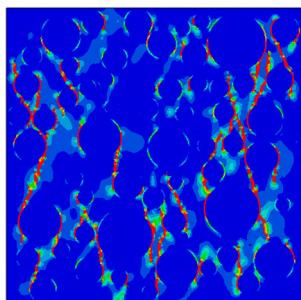
In order to better observe crack propagation and development, the concrete compression failure process was obtained with different stages of displacement, as shown in Table 4. Three typical stages were selected for the recycled concrete from initial damage to failure, namely, when damage first appears, peak strain, and destruction. First, minor circular arc-shaped damage appeared in the interface transition zone when the displacement was -0.0168 mm. Then, damage to the mortar matrix developed and the damage in small areas was connected as the displacement increased to the concrete's peak strain. Finally, the damaged crack gradually widened and the specimen was destroyed when the displacement reached -0.03 mm.

The initial damage to the RB-100 sample occurred in the interface transition zone with weak mechanical properties. With the increase in loading, the two significant damage zones appeared intensively and continued to expand along the interface between aggregate and mortar. As the damage gradually developed, part of the RBCA was broken, causing the specimen to be damaged. The maximum compression damage value of the model is 0.737.

According to Figure 12 and Table 4, the damage development of RBCA concrete differs from that of ordinary concrete. RBCA concrete and ordinary concrete damage initially appear in the interface transition zone. After all the damage occurs in the transition zone of ordinary concrete, a V-shaped central damage zone is usually formed and develops towards the mortar zone. However, the damage to RBCA concrete occurred to the aggregate itself, and no central damage zone formed.

In order to better observe crack propagation and development, the concrete compression failure process was obtained with different stages of displacement, as shown in Table 4. Three typical stages were selected for the recycled concrete from initial damage to failure, namely, when damage first appears, peak strain, and destruction. First, minor circular arc-shaped damage appeared in the interface transition zone when the displacement was -0.0168 mm. Then, damage to the mortar matrix developed and the damage in small areas was connected as the displacement increased to the concrete's peak strain. Finally, the damaged crack gradually widened and the specimen was destroyed when the displacement reached -0.03 mm.

Table 4. Destruction process of the model.

Model	Loading Displacement			Damage Value
	−0.0168 mm (Damage Appears)	−0.0280 mm (Peak Strain)	−0.0300 mm (Destroy)	
RB-100				DAMAGET (Avg: 75%) 0.737 0.675 0.614 0.553 0.491 0.430 0.368 0.307 0.246 0.184 0.123 0.061 0.000
				
				

The initial damage to the RB-100 sample occurred in the interface transition zone with weak mechanical properties. With the increase in loading, the two significant damage zones appeared intensively and continued to expand along the interface between aggregate and mortar. As the damage gradually developed, part of the RBCA was broken, causing the specimen to be damaged. The maximum compression damage value of the model is 0.737.

The damage to the RB-50 sample first appeared in the interfacial transition zone and mortar matrix, then a V-shaped central damage zone appeared. Then, the damage began to concentrate as the load displacement increased, forming three prominent damage zones. Finally, the damage zone penetrated through the whole specimen, and the specimen was further damaged as the three main damage zones continued to develop. The maximum compression damage value of the model is 0.737.

The initial damage to the RB-0 sample occurred in the interfacial transition zone. It was observed that multiple damage zones expanded along the interface between the aggregate

and mortar with increasing displacement load. Then, the damage was connected and formed a V-shaped damage zone as the load continued to develop. Finally, the cracking became larger and larger and the concrete was damaged under continuously increasing external loading. The maximum compression damage value of the model is 0.737.

The internal cracks are discrete when the RBCA substitution rate is low, and there is no apparent continuous crack formation in the section. However, the internal crack width positively correlates with the aggregate substitution rate, and one or two oblique continuous failure cracks are formed in the section. Most of the cracks are concentrated in dense areas of recycled aggregate.

3.5. The Impact of RCA Replacement Rate

The representative stress–strain curves were determined by the elastic phase, the stress–strain peak, and the curve descent section. The four characteristic indexes of compressive strength (σ), peak strain (ϵ), elastic modulus (E), and the ratio of ultimate strain to peak strain (ϵ_u/ϵ) were selected to determine the concrete constitutive curve. The constitutive curve includes three significant parameters: the maximum stress value, the straight line in the elastic stage, and the endpoint of the falling section of the curve. The ultimate strain corresponds to 0.85 times the maximum stress after the peak. The elastic modulus is the secant modulus between the origin and 0.4 times the maximum stress [29].

According to the stress–strain relationship curve obtained by numerical simulation, the compressive strength (σ), peak strain (ϵ), elastic modulus (E), and ultimate strain ratio to peak strain (ϵ_u/ϵ) were studied under different RBCA substitution rates. The variation trend of compressive strength negatively correlates with the RBCA replacement rate, as shown in Figure 13a. The compressive strength of RBAC concrete with a 100% replacement rate is 28% lower than that of ordinary concrete. This reduction in strength can be attributed to the interface and the old mortar that initially existed in the RBCA. According to the research results on the compressive strength of RBCA concrete with different contents in this paper and in the previous literature [22], the elastic modulus of RB-0 is observed to be higher than that of all RBCA specimens, as shown in Figure 13b. On the other hand, the elastic modulus of RBCA concrete is 19% lower than that of ordinary concrete when the replacement rate of RBCA is 100%, which is mainly related to the low stiffness of RBCA and the interface transition zone according to the change results of the elastic modulus of RBCA concrete with different substitution rates in both this paper and in the literature [30,42,43]. Figure 13c shows that the peak strain increases when the replacement rate of recycled aggregate increases according to the evolution law of peak strain of RBCA concrete with different content, consistent with the findings in this paper and in the literature [21,30]. However, the ratio of the limit strain to peak strain decreases with increased recycled aggregate content, as shown in Figure 13d. This phenomenon indicates that ductility increases with the recycled aggregate replacement rate.

3.6. Effect of Interfacial Transition Zone Thickness

The interface transition zone is an equal-thickness thin layer between the aggregate and mortar matrix; its performance significantly impacts the mechanical properties of concrete [44]. As the incorporation of RBCA complicates the internal interface of concrete, it is necessary to analyze the thickness of the concrete interface transition zone and study the failure mechanism of RBCA concrete. This can provide a basis for studying changes in the macromechanical properties of the concrete.

The thickness of the interface transition zone is minimal; simulations performed by previous researchers with different selected interface thicknesses have considered the calculation limitation. Here, the thickness of the interface transition zone was set as 0.5 mm, 0.75 mm, and 1.0 mm, respectively [34,39]. Figure 14 shows the stress–strain relationship of RBCA concrete with different thicknesses of the interfacial transition zone in RF-100. The load–displacement curves of each group of specimens almost wholly overlap before the strength reaches 17 MPa. After the strength reaches 17 MPa, the specimens with larger

interface thickness first enter the strengthening stage, while the other specimens with smaller interface thickness remain in the elastic deformation stage. It can be observed that the slopes of the load–displacement curves of the specimens with different interface thicknesses in the elastic stage are similar. However, the elastic stage lasts longer for the specimens with smaller interface thickness. The main reason for this is that the porosity of the interface transition zone in RBCA is relatively large and its material properties are relatively weak. Therefore, the greater the thickness of the interface transition zone, the smaller the overall compressive strength of the recycled concrete specimen is, and vice versa.

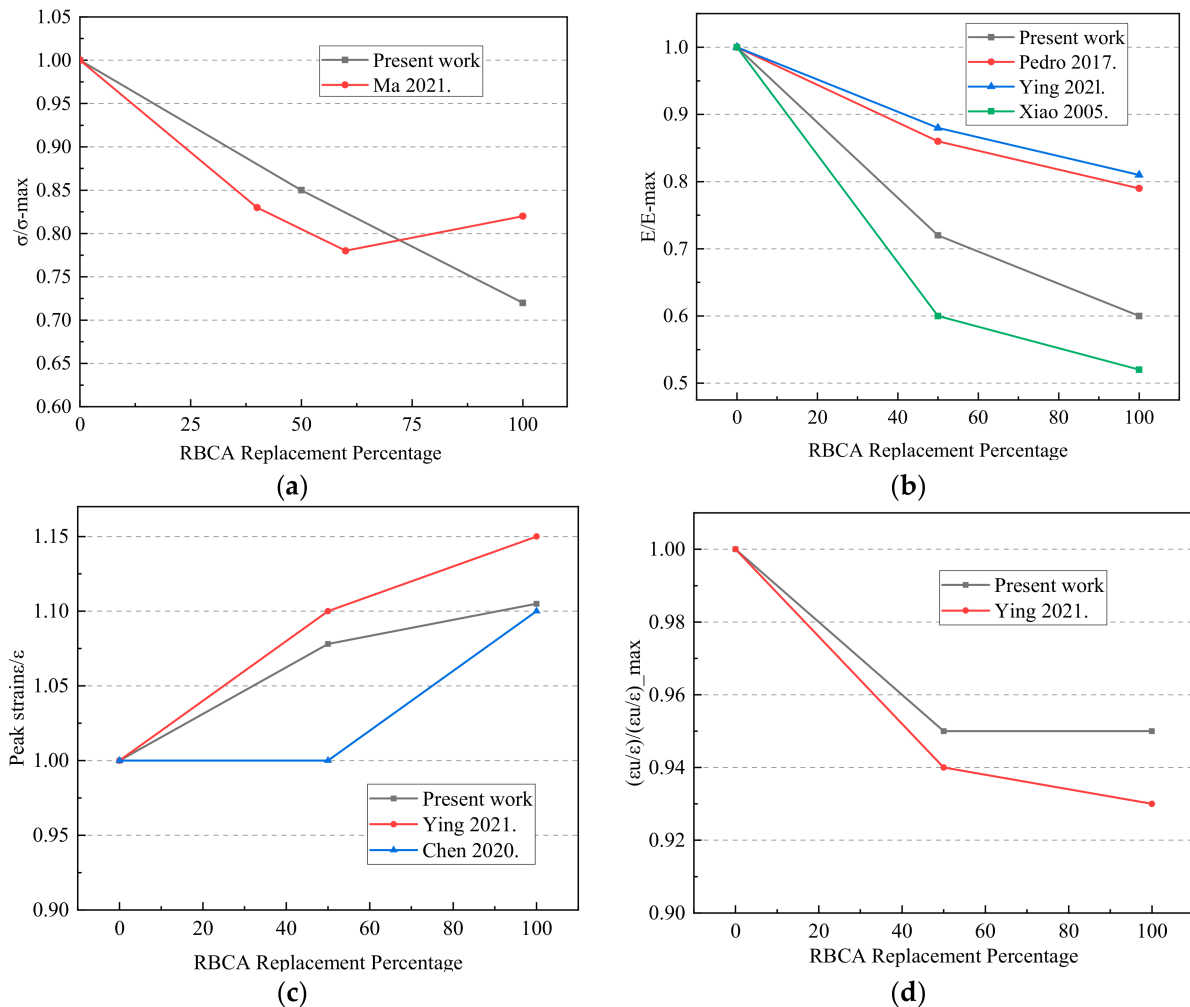


Figure 13. The effect of RCA replacement rate: (a) compressive strength, (b) elastic modulus, (c) peak strain, (d) ratio of ultimate strain to peak strain.

When the interface thickness increases from 0.5 mm to 0.75 mm, the compressive strength decreases by 8.47% and the peak strain decreases by 4.5%. When the interface thickness increases from 0.5 mm to 1 mm, the compressive strength decreases to 15.2% and the peak strain decreases by 9.5%. The concrete’s peak strain and compressive strength gradually decrease as the interfacial transition zone thickness increases. Thus, the thickness of the interfacial transition zone significantly influences the compressive strength of RBCA concrete. Figure 14 shows the stress–strain relationship of RBCA concrete with different thicknesses of the interfacial transition zone in RF-100.

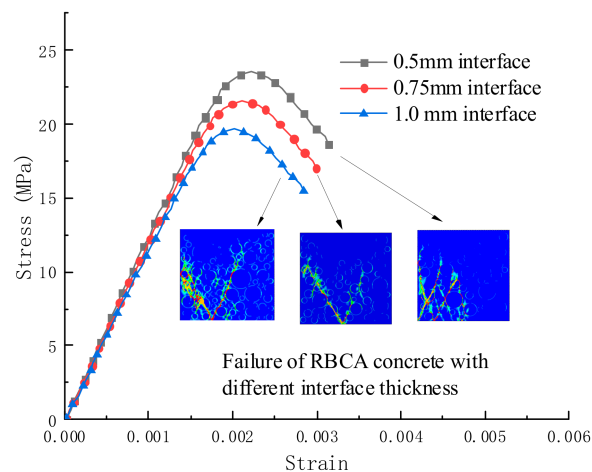


Figure 14. Stress–strain relationship of RBCA concrete with different interface thickness.

3.7. Stress Analysis

The stress distribution of RBCA concrete at peak load when subjected to uniaxial compression is shown in Figure 15; here, “+” represents tensile stress, “−” represents compressive stress, S11 is horizontal stress, S22 is vertical stress, and S12 is shear stress. Comparing the S11 stress of each model, the S11 model’s red area gradually deepens as the aggregate substitution rate increases. The red area is the largest for model RB-100, and the color is darkest, indicating that it is subject to significant transverse tensile stress. There are only a few red areas for model RB-0, and the color is scattered, indicating that the transverse tensile stress is minor. Similarly, in comparing the S22 stress of each model the red area of the model interface area decreases with increasing aggregate content. The red area of the RB-100 interface is the least, and is mainly affected by vertical compressive stress. Finally, in comparing the S12 stress of each model, all specimens have a stress distribution exerting a similar V shape. There are tensile and shear stress concentrations in the interface transition zone and aggregate edge under uniaxial compression load conditions. The tensile stress and shear stress concentration zones coincide with the damage and failure zones, failing the model requirements.

3.8. Parameters Investigation

The above analysis shows that the finite element model results are in good agreement with the experimental test results, which verifies the accuracy of the numerical simulation results. Therefore, more research on the content of RBCA was carried out using the finite element model. Recycled concrete models with five RBCA contents (0%, 20%, 40%, 60%, 80%, and 100%) were established, and the stress–strain relationships for specimens with RB-0 to Rb-100 were obtained.

Figure 16 shows the stress–strain curve of recycled concrete predicted by the finite element method. Compared with RB-0, the compressive strengths of RB-20, RB-40, RB-60, RB-80, and RB-100 concrete were reduced by 4.5%, 8.9%, 17.9%, 20.9%, and 29.8%, respectively. This is due to the generally low strength of RBCA. The elastic modulus decreased by 9.1%, 20.8%, 27.3%, 36.6%, and 39.4%, respectively, due to the more significant elastic deformation of RBCA. The peak strain increased by 2.6%, 5.2%, 10.5%, 13.1%, and 15.7%, respectively, due to the more excellent ductility of recycled concrete. It was observed that the compressive strength and elastic modulus of recycled concrete decreased with increased recycled aggregate content, and the peak strain increased with increased recycled aggregate content. Compressive strength, elastic modulus, and maximum strain are the indexes that control a material’s strength, deformation, and ductility. Through these three indexes, a detailed and comprehensive understanding of the mechanical properties of concrete can be obtained. Our results show that adding RBCA with low mechanical

properties into concrete reduces the strength of concrete to a certain extent, while the elastic deformation and ductility are improved.

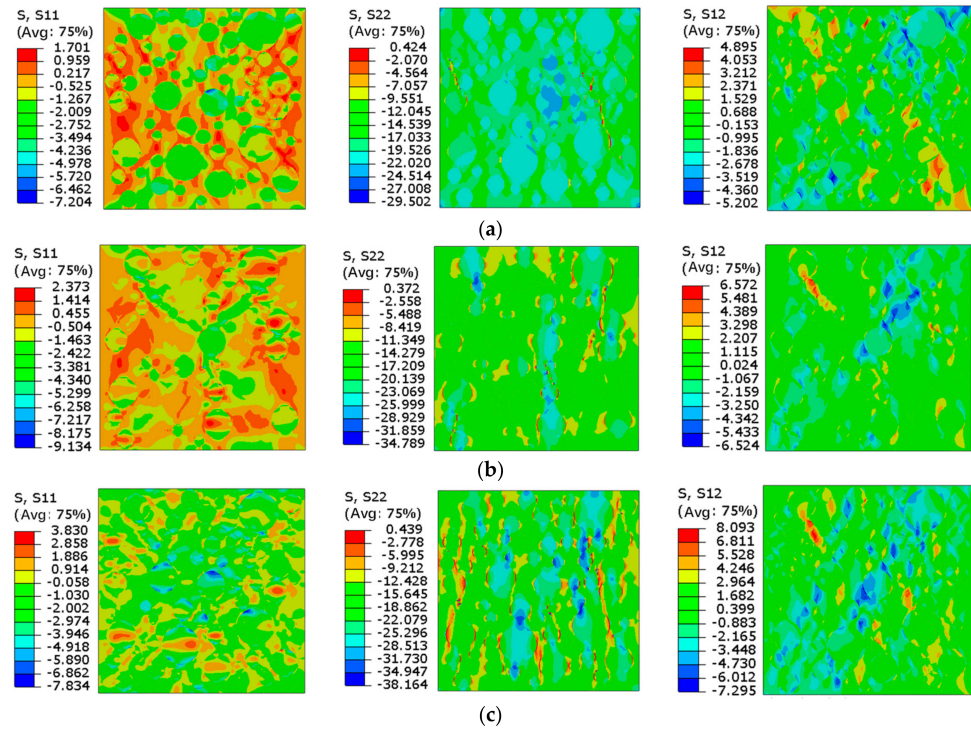


Figure 15. Stress state at peak strain: (a) RB-100, (b) RB-50, (c) RB-0.

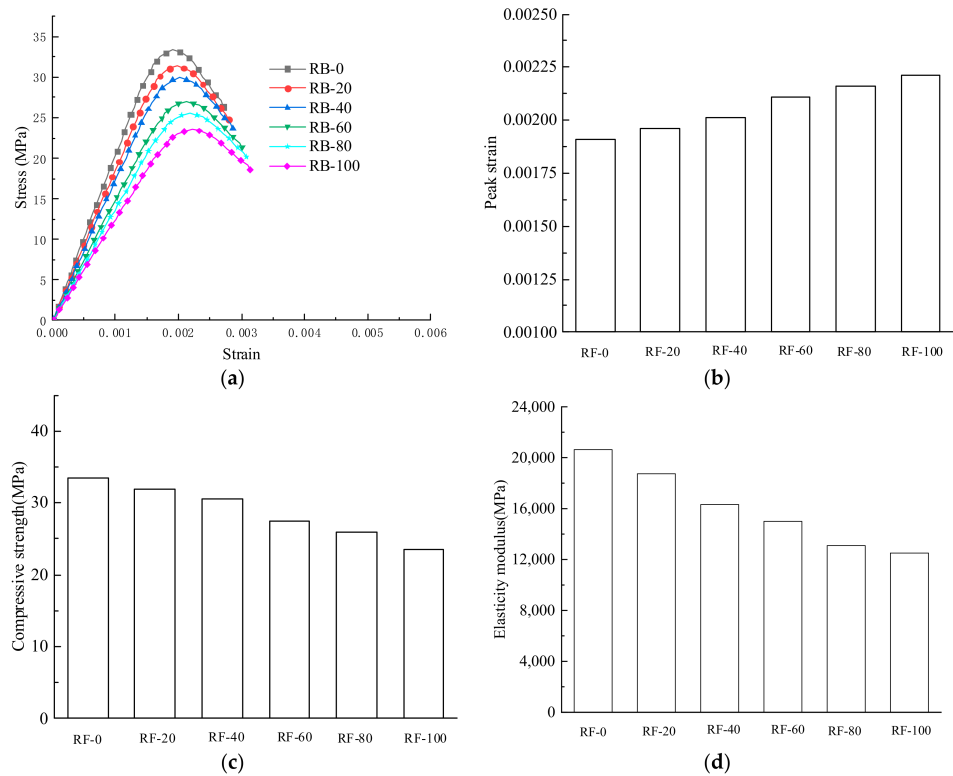


Figure 16. Finite element prediction results of concrete with different RBCA content: (a) stress–strain curve, (b) histogram of peak strain, (c) histogram of compressive strength, (d) histogram of elasticity modulus.

4. Conclusions

In order to study the mechanical and microscopic properties of RBCA concrete, the slump, apparent density, and compressive strength of RBCA concrete with different contents were tested in this paper. Combined with numerical analysis, the damage mechanism of the finite element model was studied and the content of RBCA and the thickness of the interface transition zone were analyzed, resulting in the following conclusions:

- (1) Replacement of NCA with RBCA reduces the weight of concrete. Our experimental results show that when the RBCA content in concrete was 25%, 50%, 75%, and 100%, the apparent density of concrete was 3.95%, 7.52%, 10.46%, and 15.55% lower than that of ordinary concrete. In addition, replacing NCA with RBCA reduces the fluidity of concrete. The slump decreases significantly with increasing RBCA replacement rate, although this effect decreases significantly when the replacement rate is less than 50%.
- (2) Compared with ordinary concrete, the reduction rate of the compressive strength of 25%, 50%, 75%, and 100% RBCA concrete were 5.7%, 14%, 20.6%, and 28.6%, respectively, the peak strain of the concrete increased by 2.5%, 7.5%, 10.5%, and 15.0%, respectively, and the elastic modulus decreased by 10.4%, 18.9%, 27.4%, and 38.5%, respectively. Focusing on the compressive strength of RBCA concrete and taking into account the workability of fresh concrete and the principle of improving the utilization rate of RBCA, the best replacement rate is 25%.
- (3) The failure process of recycled concrete was predicted by numerical simulation. When the replacement rate of RBCA is 100%, 1~2 oblique continuous failure cracks form on the section. When the replacement rate of RBCA is 0~50%, the internal cracks are relatively discrete. The stress state of RBCA concrete under peak strain was obtained by numerical analysis. Tensile stress and shear stress concentration exist in the interface transition zone and the edge of the aggregate. The concentrated tensile and shear stress area coincides with the damage and failure area, failing the model requirements.
- (4) The compressive strength, peak strain, elastic modulus, and ratio of ultimate strain to peak strain were studied for different RBCA substitution rates. The compressive strength, tensile strength, and initial elastic modulus decreased with increased RCA content, while the peak strain increased slightly.
- (5) Based on the numerical model, the effects of the thickness of the interface transition zone and the replacement rate of recycled aggregate on the compressive strength of recycled concrete were studied. The substitution rate of RBCA and the thickness of the interfacial transition zone negatively correlate with compressive strength and positively correlate with elastic modulus and peak stress.

Author Contributions: Conceptualization, Y.J. and L.W.; methodology, D.W.; software, D.W.; validation, Y.J., L.W. and D.W.; formal analysis, D.W.; investigation, L.W.; resources, Y.J.; data curation, Y.J.; writing—original draft preparation, D.W.; writing—review and editing, Y.J.; visualization, D.W.; supervision, Y.J.; project administration, Y.J.; funding acquisition, Y.J. All authors have read and agreed to the published version of the manuscript.

Funding: This research was funded by the Fundamental Research Funds for the Central Universities (No. 2572022BJ03) and the Heilongjiang Province Studying Abroad Student (Startup Class) Scholarships.

Institutional Review Board Statement: Not applicable.

Informed Consent Statement: Not applicable.

Data Availability Statement: All data generated or analyzed during this study are included in this published article.

Acknowledgments: The authors would like to acknowledge support from the Fundamental Research Funds for the Central Universities (No. 2572022BJ03) and the Heilongjiang Province Studying Abroad Student (Startup Class) Scholarships.

Conflicts of Interest: The authors declare no conflict of interest.

References

1. Cheng, B.C.; Tao, J.; Huang, Q.W.; Wu, H.Z.; Ding, Q.Z.; Zhan, Y.W. Summary of Research on Ultra High Performance Concrete. *J. Build. Sci. Eng.* **2014**, *31*, 1–24.
2. Zhongyan Puhua Research Institute. *2022–2027 China Concrete Industry Market In-depth Research and Investment Strategy Forecast Report*; Zhongyan Puhua Research Institute: Shenzhen, China, 2022.
3. Liu, F.; Liu, J.; Ma, B.; Huang, J.; Li, H. Basic properties of concrete incorporating recycled ceramic aggregate and ultra-fine sand. *J. Wuhan Univ. Technol.-Mater. Sci. Ed.* **2015**, *30*, 352–360. [[CrossRef](#)]
4. Zhang, Y.; Zhao, Z.; Liu, L.X. Finite element numerical analysis of precast wall panels made of waste bricks and recycled concrete under reciprocating loads. *Build. Sci.* **2016**, *32*, 101–106.
5. Zhu, M.Q. *Experimental Study on the Mix Ratio and Basic Mechanical Properties of Recycled Brick-Aggregate Concrete*; Xi'an University of Architecture and Technology: Xi'an, China, 2020.
6. Xiao, J.Z.; Lan, Q.B.; Zhang, Q.T.; Zhang, K.J. Application and prospect of combined recycled concrete and its derived structures. *J. Build. Sci. Eng.* **2022**, 1–18.
7. Poon, C.S.; Chan, D. Paving blocks made with recycled concrete aggregate and crushed clay brick. *Constr. Build. Mater.* **2006**, *20*, 569–577. [[CrossRef](#)]
8. Cheng, G.; Zhang, K.S.; Kou, S.C.; Pan, Z.S. Effects of typical construction solid waste recycled aggregates on the performance of environmentally friendly bricks. *J. Environ. Eng.* **2013**, *7*, 2716–2720.
9. Li, L.S.; Peng, Y.L.; Gong, A.M.; Song, T.W. Analysis of the influence of different replacement rates of recycled coarse aggregate on the workability and strength of concrete. *Concrete* **2007**, *8*, 41–43.
10. Deng, X.H.; Lu, Z.L.; Li, P.; Xu, T. An Investigation of Mechanical Properties of Recycled Coarse Aggregate Concrete. *Arch. Civ. Eng.* **2016**, *62*, 19–32. [[CrossRef](#)]
11. Xuan, D.; Zhan, B.; Poon, C.S. Development of a new generation of eco-friendly concrete blocks by accelerated mineral carbonation. *J. Clean. Prod.* **2016**, *133*, 1235–1241. [[CrossRef](#)]
12. Bao, J.; Li, S.; Zhang, P.; Ding, X.; Xue, S.; Cui, Y.; Zhao, T. Influence of the incorporation of recycled coarse aggregate on water absorption and chloride penetration into concrete. *Constr. Build. Mater.* **2020**, *239*, 117845. [[CrossRef](#)]
13. Sheen, Y.N.; Wang, H.Y.; Juang, Y.P.; Le, D.H. Assessment on the engineering properties of ready-mixed concrete using recycled aggregates. *Constr. Build. Mater.* **2013**, *45*, 298–305. [[CrossRef](#)]
14. Awall, M.; Oli-Ur-Rahaman, M.; Azad, M.; Rabbi, S.F. Compressive strength behavior of concrete by partial replacement of regular brick with over-burnt brick aggregate. *Innov. Infrastruct. Solut.* **2017**, *2*, 11. [[CrossRef](#)]
15. Silva, Y.F.; Robayo, R.A.; Matthey, P.E.; Delvasto, S. Properties of self-compacting concrete on fresh and hardened with residue of masonry and recycled concrete. *Constr. Build. Mater.* **2016**, *124*, 639–644. [[CrossRef](#)]
16. Bheel, N.; Kumar, K.R.; Kumar, A.; Bhagam, R.; Adesina, A.; Meghwar, S.; Memon, N.A. Innovative use of brick wastes as coarse aggregate in concrete. In *IOP Conference Series: Materials Science and Engineering*; IOP Publishing: Bristol, UK, 2020; Volume 981, p. 032077.
17. Zhang, S.; Zong, L. Properties of concrete made with recycled coarse aggregate from waste brick. *Environ. Prog. Sustain. Energy* **2014**, *33*, 1283–1289. [[CrossRef](#)]
18. Poon, C.S.; Shui, Z.H.; Lam, L.; Fok, H.; Kou, S.C. Influence of moisture states of natural and recycled aggregates on the slump and compressive strength of concrete. *Cem. Concr. Res.* **2004**, *34*, 31–36. [[CrossRef](#)]
19. Agrela, F.; De Juan, M.S.; Ayuso, J.; Geraldés, V.L.; Jiménez, J.R. Limiting properties in the characterisation of mixed recycled aggregates for use in the manufacture of concrete. *Constr. Build. Mater.* **2011**, *25*, 3950–3955. [[CrossRef](#)]
20. Yang, J.; Du, Q.; Bao, Y. Concrete with recycled concrete aggregate and crushed clay bricks. *Constr. Build. Mater.* **2011**, *25*, 1935–1945. [[CrossRef](#)]
21. Chen, J.; Geng, Y.; Wang, Y.; Sun, W. Basic mechanical properties and stress-strain relationship of recycled concrete containing broken red bricks. *J. Build. Struct.* **2020**, *41*, 184–192.
22. Ma, K.; Huang, X.Y.; Hu, M.; Peng, L.; Zhang, X. Damage Constitutive Relationship of Brick-concrete Recycled Coarse Aggregate Concrete. *J. Build. Mater.* **2021**, *25*, 1–15.
23. Hu, X.; Lu, Q.; Xu, Z.; Zhang, W.; Cheng, S. Compressive stress-strain relation of recycled aggregate concrete under cyclic loading. *Constr. Build. Mater.* **2018**, *193*, 72–83. [[CrossRef](#)]
24. Wei, H.; Tao, Y.; Yan, C.; Pei, G.; Lang, Z. Study on Damage Constitutive Model of Recycled Aggregate Concrete in Code for Design of Concrete Structures and Development in Abaqus. *J. Phys. Conf. Ser. IOP Publ.* **2021**, *1759*, 012002. [[CrossRef](#)]
25. Peng, J.L.; Du, T.; Zhao, T.S.; Song, X.Q.; Tang, J.J. Stress-Strain Relationship Model of Recycled Concrete Based on Strength and Replacement Rate of Recycled Coarse Aggregate. *J. Mater. Civ. Eng.* **2019**, *31*, 04019189. [[CrossRef](#)]
26. Wittmann, F.H.; Roelfstra, P.E.; Sadouki, H. Simulation and analysis of composite structures. *Mater. Sci. Eng.* **1985**, *68*, 239–248. [[CrossRef](#)]
27. Zhou, H.P.; Peng, Y.J.; Dang, N.N.; Pu, J.W. Numerical simulation of uniaxial compression performance for recycled concrete using micromechanics. In *Applied Mechanics and Materials*; Trans Tech Publications Ltd.: Wollerau, Switzerland, 2013; Volume 253, pp. 550–554.
28. Jayasuriya, A.; Adams, M.P.; Bandelt, M.J. Generation and numerical analysis of random aggregate structures in recycled concrete aggregate systems. *J. Mater. Civ. Eng.* **2020**, *32*, 04020044. [[CrossRef](#)]

29. Liu, Q.; Xiao, J.Z.; Li, W.G. Axial Tensile Performance Test and Lattice Numerical Simulation of Recycled Concrete. *J. Sichuan Univ. (Eng. Sci. Ed.)* **2010**, *42* (Suppl. S1), 119–124.
30. Ying, L.; Peng, Y.; Kamel, M.M. A 3-D base force element method on meso-damage analysis for recycled concrete. *Struct. Concr.* **2021**, *23*, 1962–1980. [[CrossRef](#)]
31. Yang, H.F.; Deng, Z.H.; Hu, Y.F. Microstructure and finite element analysis of recycled aggregate concrete. In *Applied Mechanics and Materials*; Trans Tech Publications Ltd.: Wollerau, Switzerland, 2013; Volume 357, pp. 1383–1388.
32. Peng, Y.; Chu, H.; Pu, J. Numerical simulation of recycled concrete using convex aggregate model and base force element method. *Adv. Mater. Sci. Eng.* **2016**, *2016*, 5075109. [[CrossRef](#)]
33. Kosmatka, S.H.; Kerkhoff, B.; Panarese, W.C. *Design and Control of Concrete Mixtures*; Portland Cement Association: Skokie, IL, USA, 2002.
34. Duan, D.X. *Research on Mechanical Properties of Recycled Concrete Based on Mesostructured*; Xi'an University of Technology: Xi'an, China, 2018.
35. Lee, J.; Fenves, G.L. Plastic-damage model for cyclic loading of concrete structures. *J. Eng. Mech.* **1998**, *124*, 892–900. [[CrossRef](#)]
36. Liu, Q.D.; Zhang, X.L.; Qin, W.P.; Zheng, Y.W.; Chen, Q.F. Research on Strengthening and Application of Recycled Aggregate of Waste Bricks. *Concrete* **2018**, *2*, 42–45.
37. Zhang, X.B. *Research on Modification and Mix Design of Recycled Concrete*; Hunan University: Changsha, China, 2015.
38. Zhang, X.Y. Research on Application of Recycled Aggregate in High Performance Concrete. *Concrete* **2017**, *2*, 87–90+94.
39. Jin, L.; Yang, W.X.; Yu, W.X.; Du, X.L. Analysis of Dynamic Compression Failure and Size Effect of Lightweight Aggregate Concrete Based on Mesoscopic Simulation. *Eng. Mech.* **2020**, *37*, 56–65.
40. Ge, Z.; Wang, Y.; Sun, R.; Wu, X.; Guan, Y. Influence of ground waste clay brick on properties of fresh and hardened concrete. *Constr. Build. Mater.* **2015**, *98*, 128–136. [[CrossRef](#)]
41. Mansur, M.A.; Wee, T.H.; Cheran, L.S. Crushed brick as coarse aggregate for concrete. *ACI Mater. J.* **1999**, *96*, 478–484.
42. Xiao, J.; Li, J.; Zhang, C. Mechanical properties of recycled aggregate concrete under uniaxial loading. *Cem. Concr. Res.* **2005**, *35*, 1187–1194. [[CrossRef](#)]
43. Pedro, D.; De Brito, J.; Evangelista, L. Structural concrete with simultaneous incorporation of fine and coarse recycled concrete aggregates: Mechanical, durability and long-term proper-ties. *Construct Build Mater.* **2017**, *154*, 294–309. [[CrossRef](#)]
44. Ghanem, H.A.; Phelan, S.; Senadheera, S.; Pruski, K. Chloride Ion Transport in Bridge Deck Concrete under Different Curing Durations. *ASCE J. Bridge Eng.* **2008**, *13*, 218–225. [[CrossRef](#)]